JOURNAL GEOLOGICAL SOCIETY OF INDIA
Vol.78, August 2011, pp.99-108

Prediction of Sea Ice Edge in the Antarctic Using GVF Snake Model

Pravin K. Rana[+], Mihir K. Dash*, A. Routray* and P. C. Pandey*
[+] Royal Institute of Technology, Stockholm, Sweden
* Indian Institute of Technology, Kharagpur, India
Email: mihir@coral.iikgp.ernet.in

Abstract: Antarctic sea ice cover plays an important role in shaping the earth's climate, primarily by insulating the ocean from the atmosphere and increasing the surface albedo. The convective processes accompanied with the sea ice formation result bottom water formation. The cold and dense bottom water moves towards the equator along the ocean basins and takes part in the global thermohaline circulation. Sea ice edge is a potential indicator of climate change. Additionally, fishing and commercial shipping activities as well as military submarine operations in the polar seas need reliable ice edge information. However, as the sea ice edge is unstable in time, the temporal validity of the estimated ice edge is often shorter than the time required to transfer the information to the operational user. Hence, an accurate sea ice edge prediction as well as determination is crucial for fine-scale geophysical modeling and for near-real-time operations. In this study, active contour modelling (known as Snake model) and non-rigid motion estimation techniques have been used for predicting the sea ice edge (SIE) in the Antarctic. For this purpose the SIE has been detected from sea ice concentration derived using special sensor microwave imager (SSM/I) observations. The 15% sea ice concentration pixels are being taken as the edge pixel between ice and water. The external force, gradient vector flow (GVF), of SIE for total the Antarctic region is parameterised for daily as well as weekly data set. The SIE is predicted at certain points using a statistical technique. These predicted points have been used to constitute a SIE using artificial intelligence technique, the gradient vector flow (GVF). The predicted edge has been validated with that of SSM/I. It is found that all the major curvatures have been captured by the predicated edge and it is in good agreement with that of the SSM/I observation.

Keywords: Sea ice modelling, Sea ice edge, Snake model, Antarctica.

INTRODUCTION

Antarctica, the southernmost icy continent, remains a paradise to the researchers for its vast ice sheet, extremely dynamic sea ice environment and above all its extreme weather and climate. Antarctica is often called a pulsating continent because its' ice pack (i.e. sea ice) grows from an area of 1.8 million km^2 by the end of austral summer, to about 20 million km^2 by the end of austral winter (Vyas et al. 2003). The total sea ice area in the Southern Hemisphere is nearly 10 times greater in the austral spring than in the austral fall. On average the advancement of ice is most rapid in the autumn from April to June and continues until late winter/early spring. Ice retreat is most rapid in the early summer of the year with minimum ice extent during February. The change in the sea ice area is due to (i) the polar location of the continent which has an almost 4 month long winter and 4 months of continuous summer (ii) the oceanic and the atmospheric circulation in this region.

Extremely dynamic sea-ice cover plays an important role in the Earth's climate system, primarily by insulating the ocean from the atmosphere and increasing the surface albedo. Fresh snow cover on ice has an albedo of the order 98% (Vowinckell and Orwing, 1970) compared to 10-15% of that of open water (Lamb, 1982). Atmospheric heat exchange over sea ice is up to two orders of magnitude less than that over Open Ocean. Seasonally expanding and contracting sea ice profoundly impedes the exchange of heat, momentum, and gases between ocean and atmosphere. Both the insulation and the albedo effects provide positive feedback and influence the local weather and climate in long run. Also, the Antarctic sea ice zone is habitat for many species of biota. Regions covered by sea ice also play an important role in specialized human activities in the Antarctic. Antarctica has no indigenous people, but several thousand people live on Antarctica during parts of the year, supporting scientific research at various stations. Maitri Station (70°46'S, 11°45'E), the logistics hub of the India's Antarctic Program, is resupplied by ships each year. Thick sea ice delays the re-supply and costs more money. So, the prediction of sea ice edge not only important form the

climatic study point, but also from the point of navigation and the study of Marine Antarctic biota.

Although the satellite system, over the last four decades, have provide us a great deal of information on the broad-scale sea ice extent and its variability. But difficulties to retrieve an accurate ice edge from satellite sensor during severe weather condition, need of reliable ice edge information over the Antarctic for fine-scale geophysical modelling and near-real-time prediction of sea ice edge (SIE) for fishing, for commercial shipping activities as well as military submarine operations is very much required. The ice edge is unstable in time, hence the temporal validity of the estimated ice edge is often shorter than the time required to transfer the information to the operational users. For example the United States National Ice Centre provides biweekly information about global sea-ice condition (Haarpaintner et al. 2004).

This paper describes a model based on the artificial intelligence and statistical analysis to map and predict the Antarctic SIE. This model utilizes the sea ice concentration information over the Southern Ocean obtained form the National Snow and Ice Data Center (NSIDC) to predict the SIE.

DATA AND METHODOLOGY

Our study utilises the sea ice concentration (SIC) obtained from the National Snow and Ice Data Center, USA. These data sets are generated using the Special Sensor Microwave/Imager (SSM/I) observations using the Bootstrap Algorithm with daily varying tie-points (Comiso et al. 1997). Daily and monthly gridded data are available on the polar stereographic grid with 25km x 25 km resolution passing a plane at 70° latitude to minimize the error in reduction of area at the polar region. Daily gridded SIC has been used in our study. 15% SIC has been considered as the threshold value for defining the ice edge (Gloersen et al. 1992). The image values have been converted into grey scale intensity value which contains only two grey level values, 255 and 0. The grey level 255 is assigned to the land pixels and the pixels having SIC more than 15%. The grey level 0 is assigned to the pixels having SIC less than 15%. Output of this processing gives a grey level image data with lots of noise (Fig.1). Noisy grey level sea ice images for two different periods (i) having peak sea ice extent (1st September 2006) and (ii) having melting of sea ice (1st February 2006) is shown in Fig.1. Noises within ice covered region represent the presence of less concentration ice pixel. In order to remove noises as well as the holes inside the foreground image, the basic concept of relationship between pixels and the images were studied. The boundaries were defined through the connectivity of pixels. The image filling has been performed using flood-fill technique by specifying a background pixel as a starting point. The boundaries were determined based on the type of neighbourhood pixel specified. The filtered images for above periods are shown in Fig.2. Canny method is used to detect the sea ice edge. Figure 3 shows typical examples of the Antarctica sea ice edges for 1st September and 1st February, 2006. These images were used to parameterize the Active Contour Model (ACM).

ACM required images with white background as well

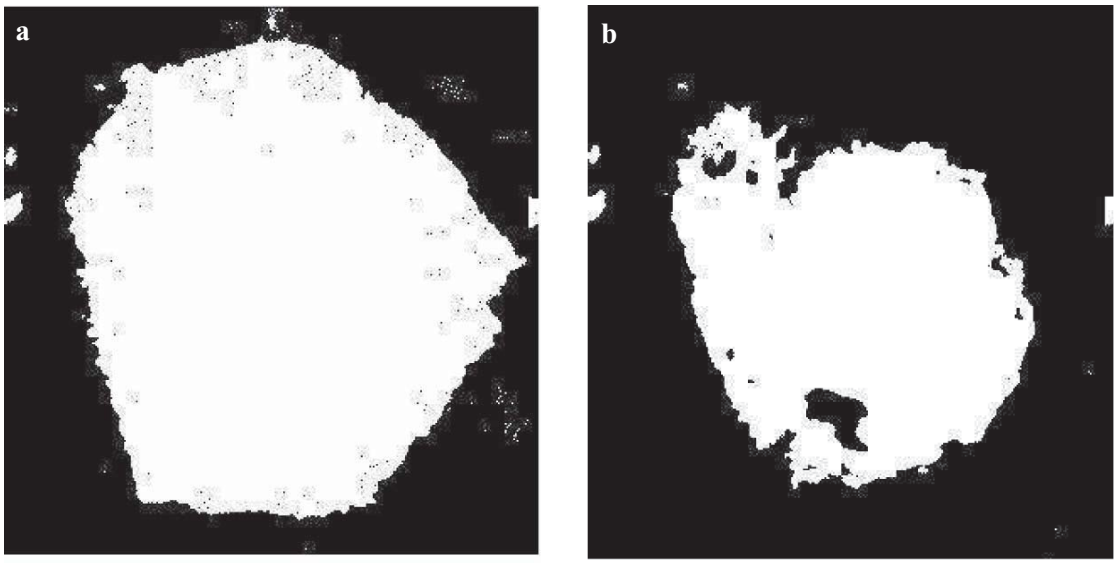

Fig.1. The grey scale of sea ice image over the Antarctic obtained after processing. The noises and hole are clearly seen in the image. **(a)** for 1st September 2006 and **(b)** for 1st February 2006.

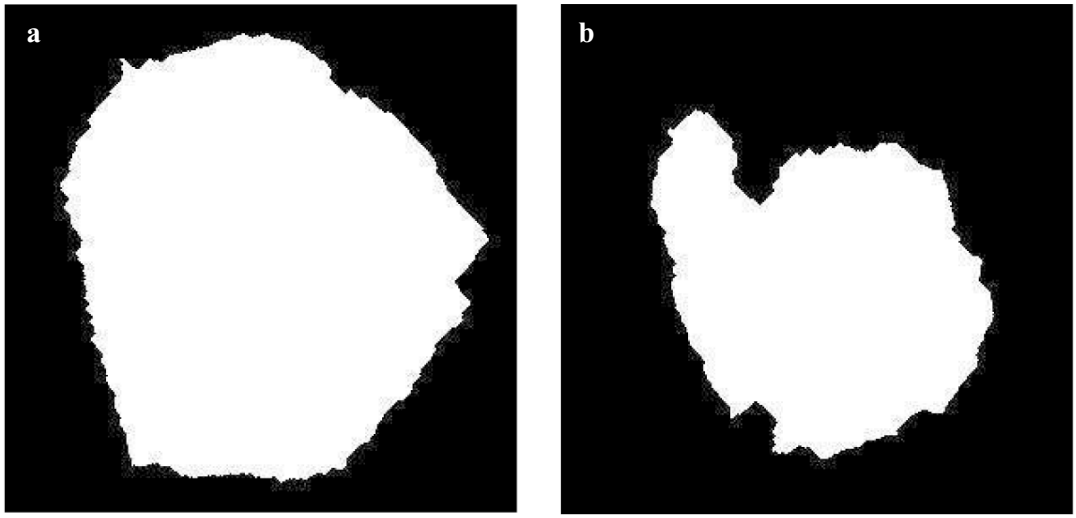

Fig.2. Processed images of the Antarctica with sea ice after the removal of noise and holes **(a)** for 1st September 2006 and **(b)** for 1st February 2006.

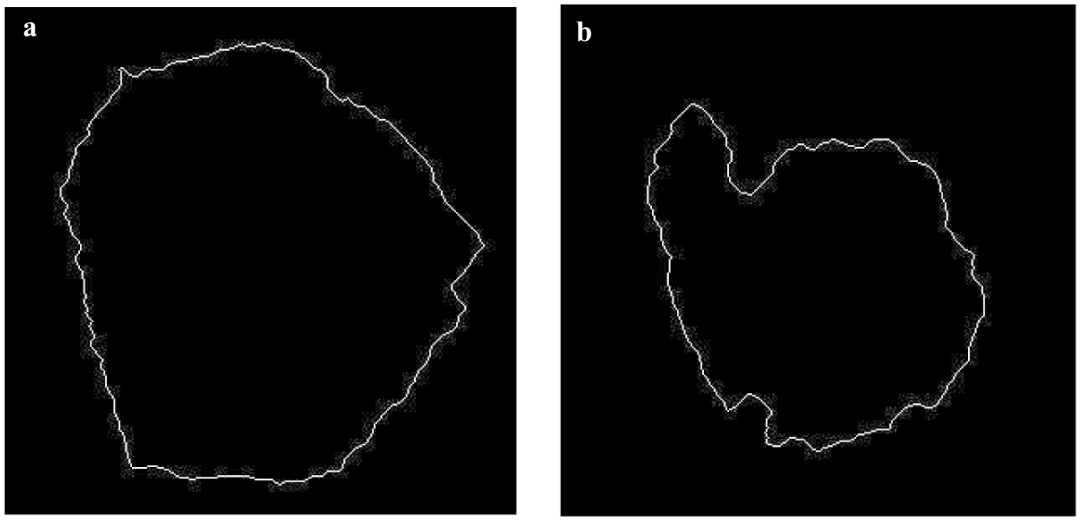

Fig.3. The edge generated using canny method from the images given in Fig 2. **(a)** for 1st September 2006 and **(b)** for 1st February 2006.

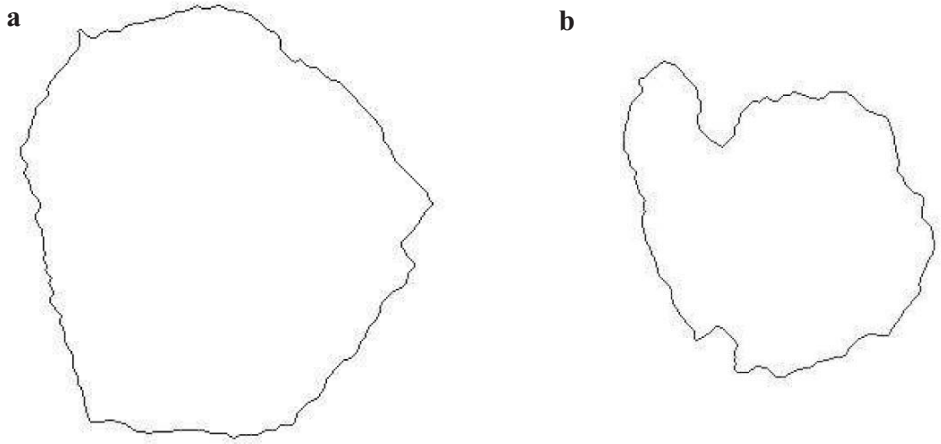

Fig.4. Sea ice edge after altering the background and foreground of the images given in Fig.3 for **(a)** September 1st, 2006 and **(b)** for February 1st, 2006. These images serve as the master to parameterize the active contours.

as PGM file format. For this purpose the image background as well as foreground gray level are changed accordingly. The resultant images with a white background and black foreground for the above two periods are shown in Fig.4.

PARAMETERIZATION OF SEA ICE EDGE USING ACTIVE CONTOUR MODEL

Sea ice edge is extremely dynamic in nature. Active Contour Model (ACM) or Snake Model is the best tool to simulate sea ice edge for prediction. This technique is extensively used in the edge detection problem and other computer vision problem like, shape recognition, object tracking and image segmentation. When edge information in the image is insufficient and corrupted by noise considerable difficulties arise in the application of classical edge detection methods for simulation of edge or boundary shape. As a result, classical techniques either fail completely or require some kind of post processing step to remove invalid object boundaries in the segmentation results. ACM promises to provide a good solution.

Mathematically, active contour is a curve defined as a function of arc length, s, is defined as $X(s) = [x(s)y(s)]$, $s \in [0,1]$ is which moves through the spatial domain of an image to minimize the following energy functional:

$$E = \int_0^1 \left\{ \frac{1}{2}\left[\alpha(s) \left| \frac{\partial X(s)}{\partial s} \right|^2 + \beta(s) \left| \frac{\partial^2 X(s)}{\partial s^2} \right|^2 \right] + E_{ext}(X(s)) \right\} ds \quad (1)$$

Where α and β are weighting parameters that control the snake's tension and rigidity, respectively (Kass et al. 1987; Cohen, 1991). The first-term represents the internal energy functional and is defined by

$$\left| \frac{\partial X(s)}{\partial s} \right|^2 \quad \text{and} \quad \left| \frac{\partial^2 X(s)}{\partial s^2} \right|^2$$

Where, $\left| \frac{\partial X(s)}{\partial s} \right|^2$ and $\left| \frac{\partial^2 X(s)}{\partial s^2} \right|^2$

denote the first and second order derivates of X(s) with respect to s. The external energy function E_{ext} is derived from image data and takes smaller values at object boundaries as well as other feature of interest. Mainly there are two different energy functions, (i) edge functional ($E^1_{ext}(x,y)$) (ii) line functional ($E^2_{ext}(x,y)$), which attract the snake or the contour. Given a grey–level image intensity of the image, I(x, y), viewed as a function of continuous position variables (x, y), typical external energy functions designed to lead an active contour toward step edge are

$$E^1_{ext}(x,y) = -\omega_e |\nabla I(x,y)|^2 \quad (2)$$

$$E^2_{ext}(x,y) = -\omega_e |\nabla [G_\sigma(x,y) * I(x,y)]|^2 \quad (3)$$

Where, ω_e is a positive weighting parameter, is a two-dimensional Gaussian function with standard deviation σ, ∇ is the gradient operator and * is the 2D image convolution operator (for detailed description of 2 and 3 please refer Kass et al. 1987; Xu and Prince, 1997). Image with a line drawing (black and white), equation 2 and 3 can be defined as follows:

$$E^3_{ext}(x,y) = \omega_l I(x,y) \quad (4)$$

$$E^4_{ext}(x,y) = \omega_l [G_\sigma(x,y) * I(x,y)] \quad (5)$$

where ω_l is a weighting parameter. Positive ω_l is used to find black lines on a white background, while negative ω_l is used to find white lines on a black background (for detailed description of 4 and 5 please refer Xu and Prince, 1997). For both edge and line potential energies, increasing σ can broaden its attraction range. However, larger σ can also cause a shift in the boundary location, resulting in a less accurate result.

INITIALIZING THE CONTOUR

For parameterization of sea ice edge over Antarctica, initial snake is defined as a circle with (166, 158) position in the image as the origin. Initial snake is taken to be a circle, because sea ice coverage over Antarctic expand/contract almost radially. The edge map was obtained by convolving the Laplacian with the image pixels. This edge map was a single channel 8 bit image. This is done because single value image intensity desired to represent the image energy. Then the Laplacian filter operated on the image and the image is converted into a single channel grey level image. The model was initialised with a circle by following equation

x = 158+105*cos(t);

y = 166+105*sin(t);

Figure 5 gives the initial circle's position on an image of Antarctica sea ice edge. Here we have shown the ice edge for 1st January 2002 which is obtained as above.

In order to increase the capture strength of the edges, the edge map was blurred so as to diffuse the effect of strong edges onto nearby pixels. As soon as any contour pixel would come within few pixel of the edge, it would start experiencing the effects of the edge and the get pulled toward the edge. A 5x5 Gaussian filter was used to achieve this blurring. Finally, armed with blurred edge map and the initial

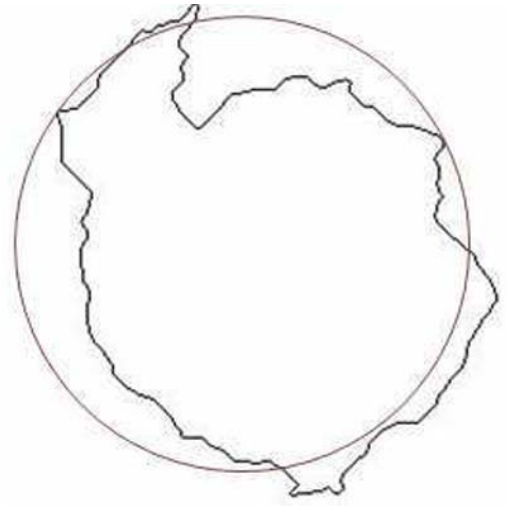

Fig.5. A typical Laplacian filtered single channel grey level image of the sea ice edge over the Antarctic with the Initial circular snake.

contour configuration is invoked which is embedded in the program.

CHOICE OF α, β, AND γ

The tension parameter of the contour α is defined at 0.2. It means that an average separation of 10 pixels between two control points should cause each to expert an elastic pull of 2 pixel on the other. Now, the bending effect is subtler. A movement of few pixels can affect the bending energy greatly. Hence, a lower value of β, the rigidity parameter is defined as 0. Furthermore, the image force needs to perform like little stronger force than the elastic force. It could be surmise as if a few points in the contour begin to drift away from an edge they should not be able to dislodge those points which have already found a good strong edge. The presence of any stray noise pixel may trap one point at a false minimum and affect the movement of snake. To avoid this situation image force should be slightly greater than elastic force. A difference of image intensity by a grey level 255 between neighbouring pixel; is considered as a transition from pure black (intensity value 0) to pure white (intensity value 255), which is the strongest edge possible. But even a difference in grey level by 100 represents a good visible edge. So we might say that an intensity gradient of 128 should exert about the same level of force as elastic force at 10 pixels apart, which is denoted by γ. This suggests a value of 1/64 for γ.

The major draw back of ACM is assigning values to the constants. After some trial and error, the values $\alpha = 0.05$, $\beta = 0$, and $\gamma = 1$ were decided upon.

GVF SNAKE METHOD

The model starts from the initial contour (circle in this case) provided to it as input. The gradient vector flow (GVF) snake (Xu and Prince, 1997) begins with the calculation of a field of forces, called the GVF forces. The field forces were calculated between different points on the initial contour and the final ice edge in steps. These forces are derived from the diffusion operations carried out in the images considering the grey values and tendency to extend very far away from the object. This extends the "capture range" so that snakes can find objects that are quite far away from the snake's initial position. The typical example of these forces over the entire image domain for the Antarctica sea ice edge is shown in Fig.6. These diffusive forces are normalized (Xu and Prince, 1997) to give the position of the contour at the end of each iteration. The output of the $(n-1)^{th}$ iteration is considered as the initial condition for the n^{th} iteration. Figure 7 shows the position of the contours at different iterations. It can be inferred from the Fig.7 that the contour intervals are not the same at each interval, because the normalised GVF force (magnitude and direction) changes with iterations. Sine the diffusion property creates force, the active contours can be pull into concave regions (see Fig.7).

The GVF forces act on both side of the edge and try to converse to the boundary (see Fig. 8). The forces inside/outside the contour represent the diffusive forces coming from inside/outside to the contour boundary. Mathematical expressions for these forces are described above. It is observed that the GVF field has a much larger capture range than traditional potential forces. A second observation is that the GVF vectors within the boundary concavity i.e. at the top of the Antarctica sea ice edge have a downward component. Finally, it can be seen in that the GVF field behaves in an analogous fashion when viewed from the inside of the object (see Fig. 8). In particular, the GVF vectors are pointing outward into Antarctica sea ice edge, which represent concavities from this perspective.

The performance of the GVF active contour model is studied on 53 weekly (corresponding to one year) sea ice concentration images with the same initial conditions and the forcing parameters (the snake parameters are chosen as: á = 0.2, â = 0.0, ë =0.3, and ã =0.4). It is found that in all the cases the model fitted to the given edge very nicely. This gives a confidence that using discrete pixel information a continuous edge can be simulated using GVF approach. This potentiality has been explored to predict the sea ice edge in the Antarctic.

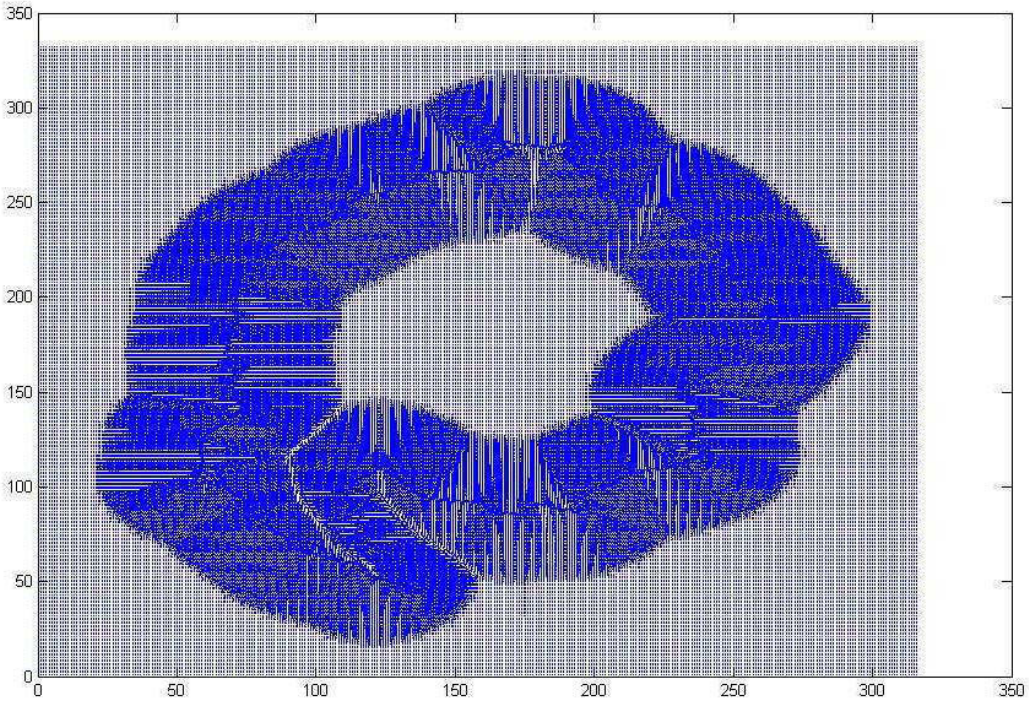

Fig.6. GVF external forces for a typical Antarctic sea ice edge image (the ice edge shown in Fig.5).

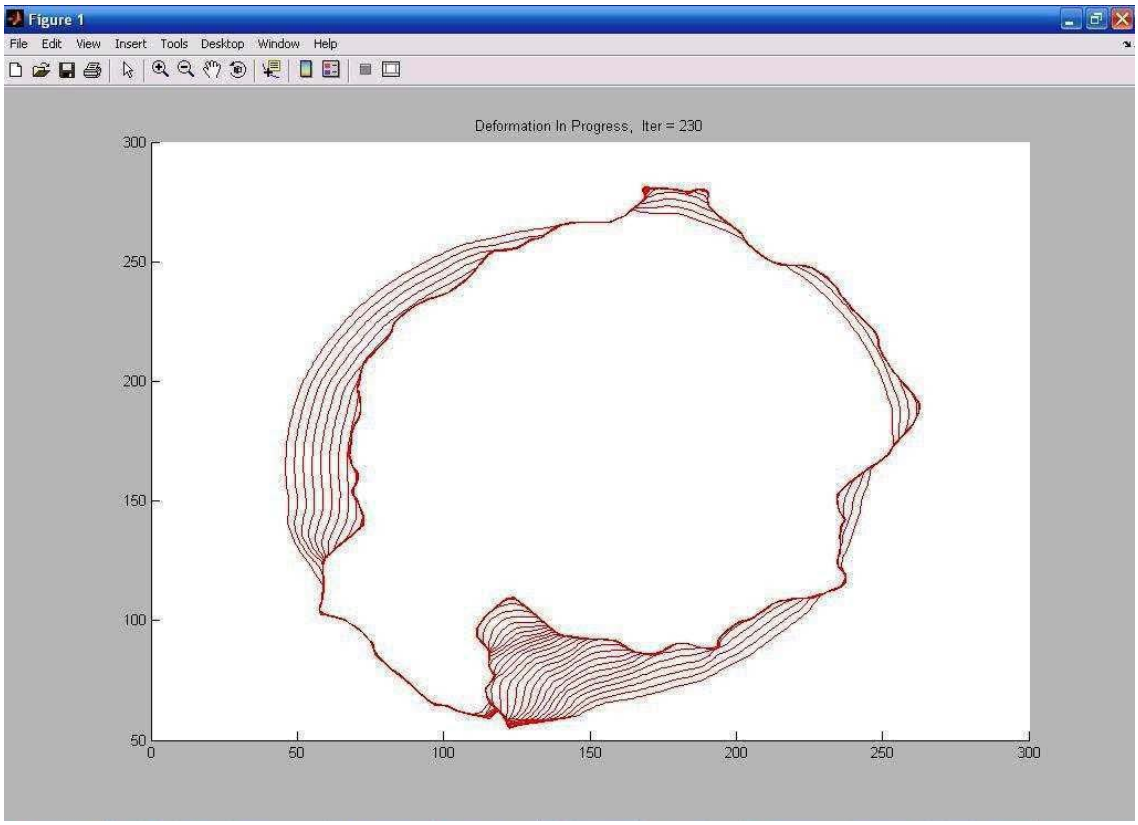

Fig.7. A view of snake deformation during a run of snake model, after 230 iterations.

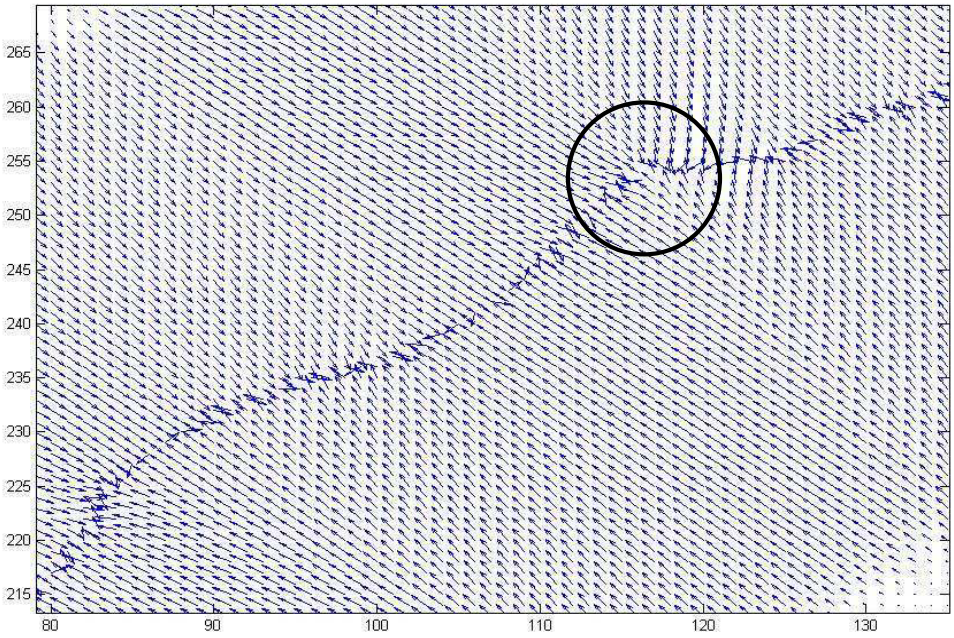

Fig.8. A close-up GVF external forces within the boundary concavity.

PREDICTION OF SEA ICE EDGE

To predict sea ice edge over Antarctic, weekly sea ice edges have been computed from the concentration images for the year 2004. The image is found to be of the form 332 pixel x 316 pixel coordinate system starting from (0, 0) at its left upper corner of the image. In this coordinate system, the image is treated as a grid of discrete elements, ordered from top to bottom and left to right. For pixel coordinates, the first component i (the row) increase downward, while the second component j (the column) increases to the right. Assuming the expansion and contraction of sea ice edge is radial, each edge pixels are transferred to radial co-ordinate system with the origin of the centre of the co-ordinate system at the pixel location (166, 158). All the edge pixels have been transformed the radial co-ordinate system using the following relation:

$$i_{new\text{-}pixel} = 166 - i_{pixel} \quad (6)$$

$$j_{new\text{-}pixel} = j_{pixel} - 158 \quad (7)$$

In the transformed co-ordinate system the radial distance of each edge pixel (r) and the angle covered (θ) with reference to the 158th row in the anti-clock wise is calculated. The relation used for the computation of the angular co-ordinate is given as follows:

$$\theta = tan^{-1}\left(\frac{i_{new-pixel}}{j_{new-pixel}}\right) \quad (8)$$

$$r = \left|\sqrt{(i_{new-pixel})^2 + (j_{new-pixel})^2}\right| \quad (9)$$

where, $i_{new\text{-}pixel}$ and $j_{new\text{-}pixel}$ are the new transformed image edge pixel in pixel coordinate system of image .

The averaged radius of edge pixels at each 1° ± 0.2 ° interval is calculated for all 53 weeks. If no ice edge is found then an undefined value (-9999.0) is assigned to the corresponding angle. In certain cases more than one solution are found for a particular angle. In this case the edge information is averaged and put as a single solution. Using the weekly data sets described above a time series of angular distribution of radius is generated. Then time series of radial variation of the edge corresponding to each angle is fitted to a four degree polynomial and a matrix with coefficients of the polynomial is generated. The equation for the matrix is given below

$$\begin{pmatrix} r_1 \\ r_2 \\ r_3 \\ r_4 \\ \vdots \\ r_{360} \end{pmatrix} = \begin{pmatrix} A_1 & B_1 & C_1 & D_1 & E_1 \\ A_2 & B_2 & C_2 & D_2 & E_2 \\ A_3 & B_3 & C_3 & D_3 & E_3 \\ A_4 & B_4 & C_4 & D_4 & E_4 \\ \vdots & \vdots & \vdots & \vdots & \vdots \\ A_{360} & B_{360} & C_{360} & D_{360} & E_{360} \end{pmatrix} \begin{pmatrix} t^4 \\ t^3 \\ t^2 \\ t \\ 1 \end{pmatrix} \quad (10)$$

with,

$$r = At^4 + Bt^3 + Ct^2 + Dt + E \quad (11)$$

where, r_θ is the radius of the each pixel locations, and θ = 1,2,3,4…, 360, each value of θ corresponds to an angles,

t is the time and A, B, C, D, E are known polynomial coefficients. Eight sample curves with 4 degree polynomial fit are shown in Fig.9.

By using coefficient matrix of polynomial equation, the radial distance of the sea ice edge 'r' at few angular positions are predicted for the time step t=55, 56. The radial components are converted back to the pixel values using the relation given below:

$$i_{New-Pixel} = rSin(\theta)$$
$$j_{New-Pixel} = rCos(\theta) \quad (12)$$

These pixel values obtained are with respect to the co-ordinate system with origin at (166,158). Again the above information is converted to the original image co-ordinate system having origin at (0,0) location. The transformation equations are given below:

$$i_{Predicted\ Pixel} = 166 - i_{New-Pixel}$$
$$j_{Predicted\ Pixel} = j_{New-Pixel} + 158 \quad (13)$$

Now, we have few predicted edge pixel position information in the image domain that can be given as input to simulate the sea ice edge. The information are put into GVF snake model and the sea ice edge is simulated using the parameters described above. After 250 iterations, snake simulates the predicted Antarctica SIE image. Figures 10 and 11 show typical GVF Snake model derived SIE image for 1st week and 2nd week of January, 2005 respectively. The corresponding SSM/I Antarctica sea ice edge image is

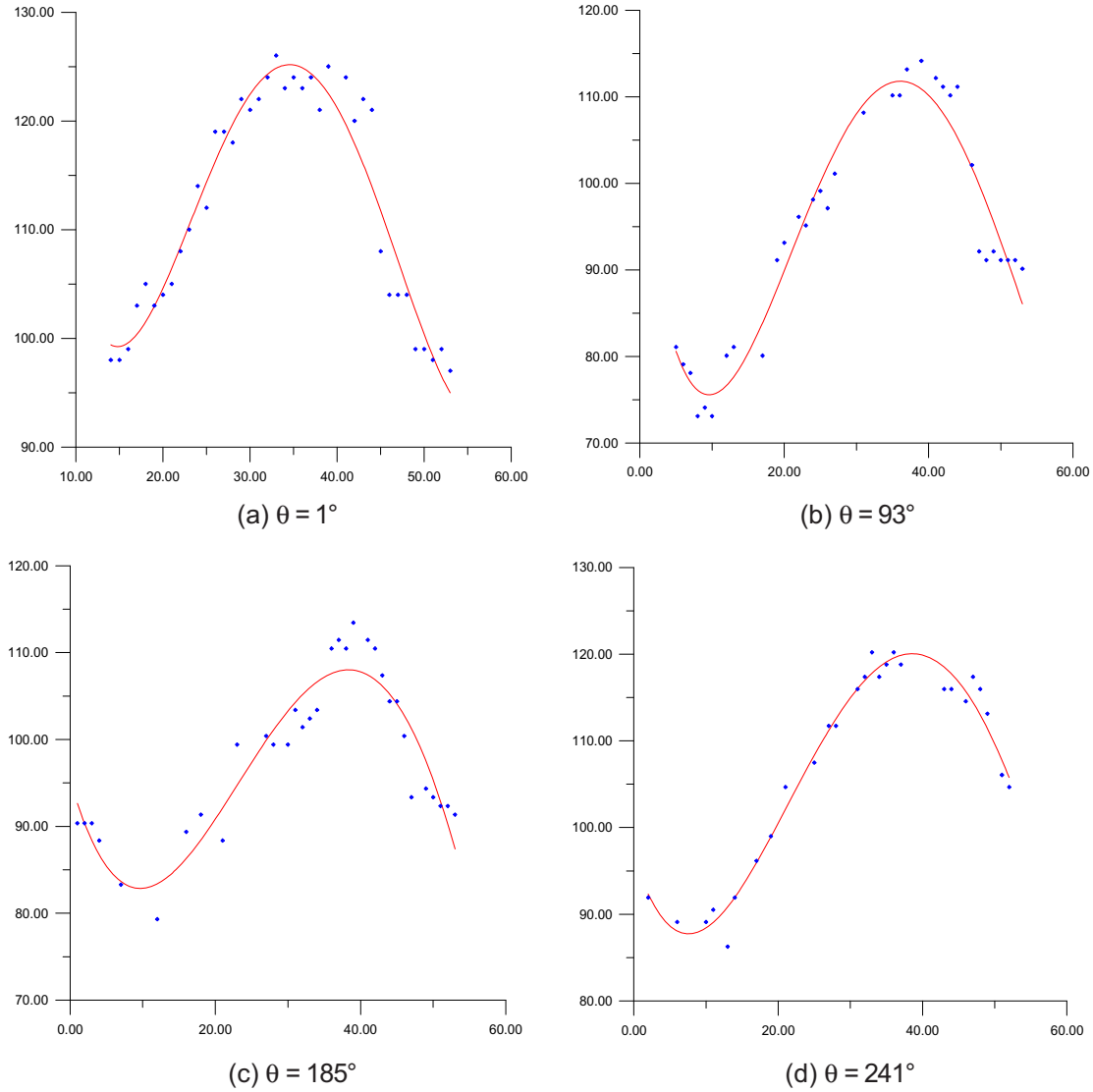

Fig.9. Typical example of 4th order polynomial curve fitting for 53 weeks, 2004 edge information data for different angles.

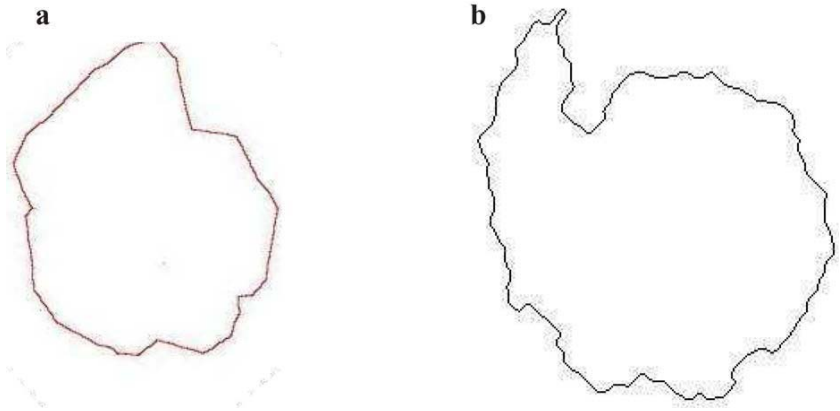

Fig.10. (a) Predicted image of 4th of January 2005 by points obtain by polynomial equation and edge simulated by point using GVF snake. **(b)** SSM/I image of the Antarctica sea ice edge of 4th January 2005 used for validation of prediction result.

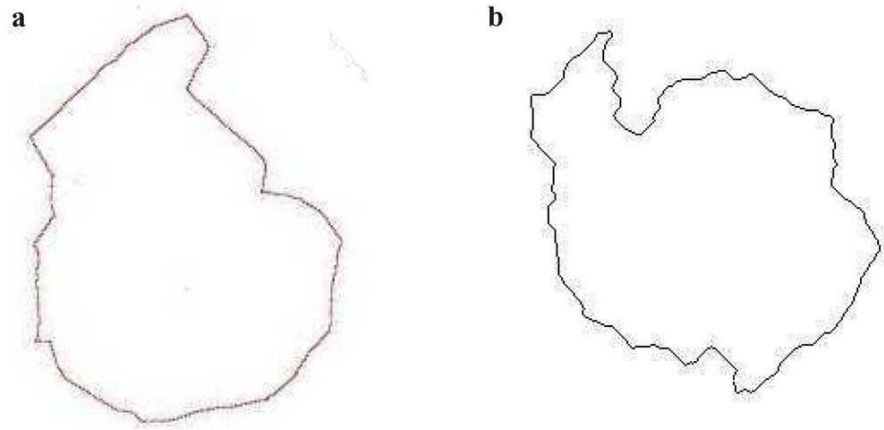

Fig.11. (a) Predicted image of 11th of January 2005 by points obtain by polynomial equation and edge simulated by point using GVF snake. **(b)** SSM/I image of the Antarctica sea ice edge of 11th January 2005 used for validation of prediction result.

also shown in these figures. This is to note that the image domain remains same as that of the polar stereographic projection image provided by NSIDC.

VALIDATION AND ERROR ANALYSIS

The predicted image validated by using Antarctica sea ice edge of same day which is obtain by SSM/I sensor. Though we trained the GVF for the 1st January 2006 and used the model parameters find out the SIE for 4th and 11th January 2005 form few predicted position of the edges. Because the model is sensitive to the initial contour provided to it and the converging points (predicted points) provided to it. The broad features of the predicted edge match well (up to 90%) with that observed edge. But there is large deviation around Antarctic peninsula. This may be due to the use of averaging technique to decide the ice edge when multiple edges are present at a particular angle. Though, less but similar error has been noticed in the Ross ice shelf region. The radial RMS error computed for both predicted image 4th January as well as 11th January of 2005 and found to be of the order of 11% for both the cases. When multiple edges are encountered along a particular radial direction this technique adds error to the prediction model.

CONCLUSIONS

From the present study it is found that the GVF snake is a robust technique to parameterize any deformable edge like the sea ice extent. Following conclusions are drawn from the parameterization of sea ice edge.

- The GVF field has a much larger capture range than traditional potential forces.
- GVF vectors fits smoothly to the boundary concavity and the GVF vectors are pointing outward into Antarctica SIE, which represent concavities.

- The GVF is insensitive to the initialization of the snake.
- The GVF field behaves in an analogous fashion when viewed from the inside of the object.
- Another observation is that the GVF snake has superior convergence properties. The final snake configuration closely approximates the true boundary, arriving at a sub pixel interpolation through bilinear interpolation of the GVF force field.

The validation of the predicted sea ice edge shows a good match with that of the observed SSM/I sea ice edge. The broad features of the predicted edge match well (up to 90%) with that observed edge. But large deviation around Antarctic peninsula is noticed. This may be due to the use of averaging technique to decide the ice edge when multiple edges are present at a particular angle. Though, less but similar error has been noticed in the Ross ice shelf region. The radial RMS error computed for both the predicted images are found to be of the order of 11%. When multiple edges are encountered along a particular radial direction this technique adds error to the prediction model. Though we have used a time series of one year for the prediction purpose, a longer time series could be used for better prediction. Also, better contour tracking methods like blocking matching method, optical flow method are under process for better prediction of the sea ice edge along a longitude.

Acknowledgements: The data used in the study are downloaded from NSIDC and NCEP/NCAR. Some of the software used are available from http://www.iacl.ece.jhu.edu/static/gvf. Financial assistance is provided by National Centre for Antarctic and Ocean Research, Goa, India.

References

Chenyang, Xu and Prince, J.L. (1997) Gradient Vector Flow: A New External Force for Snakes, Proc. IEEE Conf. on Comp. Vis. Patt. Recog. (CVPR), Los Alamitos: Comp. Soc. Press, pp.66-71, June 1997.

Cohen, L.D. (1991) Note on active contour models and balloons. CVGIP: Image Understanding, v.53, pp.211–218.

Comiso, J.C., Cavalieri, D., Parkinson, C. and Gloersen, P. (1997) Passive microwave algorithms for sea ice concentrations. Remote Sensing of the Environment, v.60, pp.357-384.

Gloerson, P., Campbe, W.J., Cavalier, D.J., Comiso, J.C., Parkinson C.L. and Zwally H.J. (1992) Arctic and Antarctic Sea Ice:178-1987. NASA-SP_511, 290p.

Kass, M., Witkin, A. and Terzopoulos, D. (1987) Snakes: The Active contour models. Internat. Jour. Computer Vision, v.1, pp.321-331.

Lamb, H.H. (1982) The climate environment of the Arctic Ocean. *In:* L. Ray (Ed.), The Arctic Ocean. John Wiley and Sons, New York, pp.135-161

Vowinckell, E. and Orwing, S. (1970) The climate in the north polar basin, climate of the polar regions. World Survey of Climatology, Elsevier, Amsterdam, v.14, pp.129-252.

Vyas, N.K., Dash, M.K., Bhandari, S.M., Khare, N., Mitra, A. and Pandey, P.C. (2003) On the secular trend in sea ice extent over the Antarctic region based on OCEANSAT – 1 MSMR Observations. Internat. Jour. Remote Sensing, v.24, pp.2277-2287.